Original Article

Mapping temporal extent of Chiang Mai floods using coupled 1-D and quasi 2-D floodplain inundation models

Kowit Boonrawd and Chatchai Jothityangkoon*

*School of Civil Engineering, Institute of Engineering,
Suranaree University of Technology, Mueang, Nakhon Ratchasima, 30000 Thailand.*

Abstract

A coupling of a 1-D flood routing model and quasi 2-D floodplain inundation model is applied for mapping space-time flood extent. The routing model is formulated based on a non-linear storage-discharge relationship which is converted from an observed and synthetic rating curve. To draw the rating curve, required parameters for each reaches are estimated from hydraulic properties, floodplain geometry and vegetation and building cover of compound channels. The shape of the floodplain is defined by using fitting exercise based on the reverse approach between past and simulated inundation flood extent, to solve the current problem of inadequate topographic input data for floodplain. Mapping of daily flood can be generated relying on flat water levels. The quasi 2-D raster model is tested and applied to generate more realistic water surface and is used to estimate flood extent. The model is applied to the floodplains of Chiang Mai, north of Thailand and used to estimate a time series of hourly flood maps. Extending from daily to hourly flood extent, mapping development provides more details of flood inundation extent and depth.

Keywords: Upper Ping River, flood map, raster model, rating curve

1. Introduction

To assess an impact of severe flood and at the same time mitigate economic and social losses, mapping of floodplain inundation extent including flood depth and flood duration is an important tool for the improvement of flood management systems. Extrapolation work from historical to future potential flood mapping under different possibilities and scenarios are necessary information for stake holders in choosing appropriate measures to reduce flood risks. The magnitude and frequency of floods possibly tend to increase in near future which is the consequence of climate and human induced changes (IPCC, 2007).

The devastating results of past floods in Chiang Mai City, particularly in the core economic and residential zones, has brought great public concern about the performance of flood protection and warning systems managed by local authorities. Questions are also being raised by the local people on what are the potential impacts of future land use changes, the forest loss to agricultural plantation, and the uncontrolled urban expansion (Chatchawan, 2005; CENDRU, 2013).

Flood inundation mapping can be formulated in a number of ways including historical flood investigation through field survey and/or remote sensing survey, using hydrological or hydraulic modeling or their combination. Compared to different approaches, hydraulic modeling gives advantages over other methods. It incorporates spatial terrain data and generates the space-time variation of flood depth and magnitudes. One dimensional (1-D) hydraulic modeling of full St. Venant equation is still a standard practice. By

receiving design flood inputs, it can simulate flood magnitude and depth downstream and convert to flood inundation extent such as MIKE, HEC (Fread, 1993; Ervine and MacLeod 1999; De Kok and Grossmann, 2010). The limitation of this method is that the map of flood inundation extent is drawn by linear interpolation of flood characteristics between each cross section. Recently, many cases of uncertainties are studied in form of probabilistic flood inundation map (Merwade *et al.*, 2008; Sarhadi *et al.*, 2012)). To overcome this limitation, two dimensional (2-D) hydraulic models have been proposed to have advantages over 1-D modeling (Horritt and Bates, 2002; Tayefi *et al.*, 2007; Cook and Merwade, 2009). Recent advances in availability of remotely sensed topographic data and high computational capability, allows 2-D flood inundation modeling based on finite difference and finite element numerical method to become practical tools to estimate floodplain inundation extent, flood depth and depth-averaged velocity vector for each node and time step (Bates and De Roo, 2000).

However, the application of the complex 2-D models require massive input data together with consuming high computational cost and time which makes this model less attractive for large-scale floodplain analysis. Application of simplified raster-based hydraulic model is widely used due to some advantages over full 2-D model to simulate dynamic flood inundation (Bradbrook *et al.*, 2004; Yu and Lane, 2006). The raster based model can simply integrate spatial topographic data and process them with high computational efficiency. These models consist of coupling the 1-D and 2-D model representing channel flow and flow over the floodplain (Bates and De Roo, 2000; Yin *et al.*, 2013). The raster-based storage model is developed further to adaptive time step diffusion model (Hunter *et al.*, 2005), including inertial term (Bates *et al.*, 2010) for high efficiency of computation with stable solutions. To improve the quality of river flood inundation prediction with given high resolution of topographic data, comparison study of different hydraulic models were examined for different topographic complexity (Tayefi *et al.*, 2007). However, scarcity of high resolution and detailed topographic data for floodplain, i.e. Lidar and synthetic aperture radar (SAR), still exists in developing countries.

2. Approaches for Floodplain Inundation Model

2.1 Storage-discharge approach

The 1-D channel routing model proposed here is based on a conceptualization of each channel link in the network as non-linear storages. The water balance of each channel reach is modeled by solving equation $dS_c/dt=I(t)-Q(t)$, combined with a non-linear storage (S_c) to discharge (Q). The storage-discharge relationship expresses as a power function $S_c = kQ^m$ where k and m are model parameters, $I(t)$ represents the summation of upstream channel reaches and lateral inflow. The parameter k and m are estimated a priori for each of the

stream reaches. These parameters reflect different physical properties of river flow transition from normal to extreme floods or from in-bank to over-bank flow (Jothityangkoon and Sivapalan, 2003; Jothityangkoon *et al.*, 2013).

For estimation of k and m in study river, recorded stage-discharge curve (rating curve) are used, together with surveyed data on the geometry of main channel, cross section of floodplain and length of the river reach. The estimation of the rating curves beyond recorded data can be achieved by a simple hydraulic approach. The compound channel is subdivided to main channels and floodplain sections, and discharges in each section are estimated separately. For the main channel, the measured rating curve can be used and estimated Manning coefficient given cross section area and slope of the channel at this stream gauge. At the other cross sections without measured rating curve, synthetic rating curves can be estimated given cross section area, slope of the channel and simulated Manning coefficient from neighbor cross section. Details of this procedure are described by Jothityangkoon and Sivapalan (2003) and Jothityangkoon *et al.* (2013). To capture the effect of houses and other buildings on the floodplain, the flow resistance in floodplain due to its size and spacing is considered in the same manner as the case of vegetation on the floodplain.

2.2 Raster based storage cell approach

(1) Diffusive model

The advantages of the storage cell formulation are that (i) it is a simple concept to calculate flow rate. Computational times and costs are much lower than solving numerical solution of full shallow water equations, (ii) this method interface well with a regular grid-based cell representing topographic characteristics generating from current remote sensing technology. For these reasons, this method is popular for floodplain inundation modeling (Hunt *et al.*, 2007). The volumetric flow rate between floodplain cells is calculated by using Manning equation,

$$Q_x^{i,j} = \frac{h_f^{5/3}}{n} \left(\frac{h^{i-1,j} - h^{i,j}}{\Delta x} \right)^{1/2} \Delta y \qquad (1)$$

where $Q_x^{i,j}$ is the flow rate in x direction at node (i, j), $h^{i,j}$ is the elevation of free water surface at node (i, j), Δx and Δy are the cell dimensions on rectangular coordinate [L], n is the Manning 's friction coefficient [L$^{-1/3}$T], h_f is the difference between the highest free water surface from two cells and the highest elevation of floodplain bed between nodes.

Interaction between inflow outflow and water surface height within a cell can be explained by water balance or continuity equation of the storage cell $\Delta h / \Delta t = \Delta Q /(\Delta x \Delta y)$. Using finite difference method, this equation is solved to,

$$\frac{^{t+\Delta t}h^{i,j} - {}^t h^{i,j}}{\Delta t} = \frac{{}^t Q_x^{i-1,j} - {}^t Q_x^{i,j} + {}^t Q_y^{i,j-1} - {}^t Q_y^{i,j}}{\Delta x \Delta y} \qquad (2)$$

where ^{t}h and $^{t+\Delta t}h$ are flow depth at time t and $t+\Delta t$, $^{t}Q_{x}^{i,j}$ is flow rate at time t and Δt is the time step.

Assuming that the depth-averaged velocity u is constant with steady and uniform flow in x direction, 1D Saint-Venant equation or momentum equation is simplified to an ordinary non-linear differential equation (neglecting acceleration and advection term),

$$S_0 + \frac{\partial h_f}{\partial x} + \frac{n^2 u^2}{h_f^{4/3}} = 0 \tag{3}$$

where S_0 is the bed slope, if flood wave propagates over flat plane, $S_0 = 0$, analytical solution can be derived (Hunter *et al.*, 2005),

$$h(x,t) = \left[\frac{7}{3} \left(C - n^2 u^2 (x - ut) \right) \right]^{\frac{3}{7}} \tag{4}$$

where h is the water depth which is a function of location on space x and at any time t, C is a constant depending on the initial condition form integration results.

(2) Inertial Model

For inertial model formulation, only advection term is neglected from 1-D Saint-Venant equation. By assuming flow in a rectangular channel a momentum equation in term of flow per unit width (q) [$L^2 T^{-1}$] is:

$$\frac{\partial q}{\partial t} + \frac{gh\partial(h+z)}{\partial x} + \frac{gn^2 q^2}{R^{4/3}h} = 0 \tag{5}$$

where z is the bed elevation [L], R is the hydraulic radius [L], g is the gravity acceleration [LT^{-2}]. For wide shallow flow, R is assumed equal h. Equation 5 can be discretize with respect to the time step Δt and q_t in the friction term is replaced by a $q_{t+\Delta t}$ (the third term in Equation 5). Equation 5 is rearranged to give flows at the next time step, derived by Bates *et al.* (2010):

$$q_{t+\Delta t} = \frac{q_t - gh_t \Delta t \frac{\partial(h_t+z)}{\partial x}}{1 + gh_t \Delta t n^2 q_t / h_t^{10/3}} \tag{6}$$

2.3 Reverse engineering approach

For some developing countries with inadequate available hydrological input data, Hagen *et al.* (2010) proposed a parsimonious model based on the reverse engineering approach to generate nationwide flood hazard maps from past inundation extents. Motivated by this study, floodplain characteristics can be defined from the map of observed flood extent and depth for lacking good quality of DEM. To evaluate the quality of flood inundation estimation, observed and simulated inundation maps are compared by considering fit index (*F*).

$$F = 100 * \left(\frac{A_{op}}{A_o + A_p - A_{op}} \right) \tag{7}$$

where A_{op} is the inundated area where both observed and simulated flood extent are completely are overlaid, A_o is the total observed area of inundation, and A_p is the total simulated area of inundation. *F* varies between zero to 100; zero means no overlap between simulated and observed inundated area and 100 means a perfect match.

3. Application to Chiang Mai Municipality

3.1 Study area

The Upper Ping River catchment is located in the north of Thailand (see Figure 1). The river flows southward through the valley of Chiang Mai. The catchment area upstream of stream gauge station P1 (Navarat Bridge) and P68 (Ban Nam Tong) are 6,350 and 6,430 km^2, respectively. The flood study area covers about half of Chiang Mai municipality (40.2km^2) and two districts (Pa Daet, 25 km^2 and Nong Hoi, 3.67 km^2) which lie on the floodplain of the Upper Ping River.

3.2 Historical flood map and flood warning system

The severe floods usually arrive during August and September. The recent ones (in the past 20 years) occurred
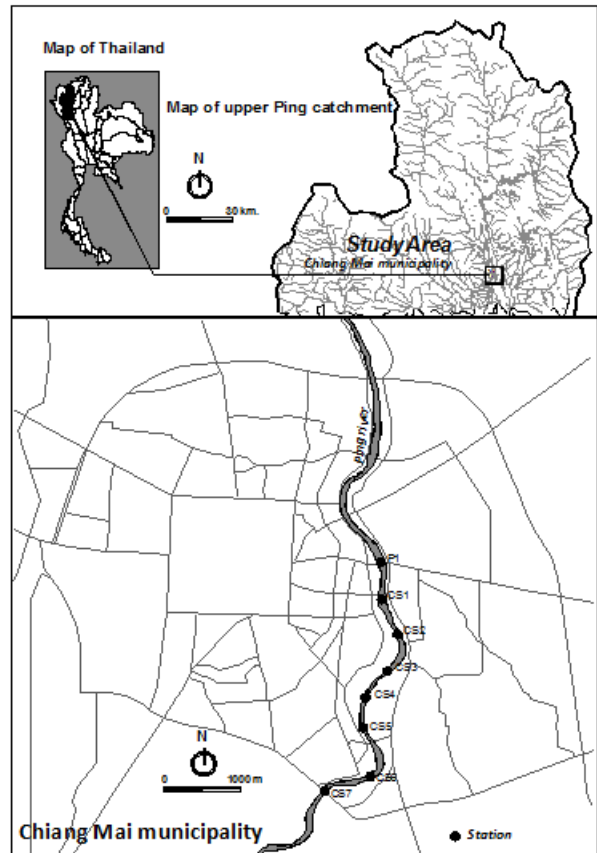
Figure 1. Location map of the Upper Ping River Basin, study reach and floodplain of Chiang Mai Municipality.

in 1994, 1995, 2001, 2005, and 2011 with maximum water levels at the P1 station of 4.43, 4.27, 4.18, 4.93 and 4.94 m, respectively. From an experience in observed flood routing from past flooding events between input flood hydrograph at stream gauge P.67 (Ban Mae Tae, 32 km upstream of P1) and output hydrograph at P1, it was found that if the maximum depth of flood at P.67 equals 4.70 m, the maximum depth of flood at P.1 equals 3.7 m, within about 7-8 hrs later (Chatchawan, 2005). Based on this correlation and observed relationship between flood level at P1 and flood depth measured in the city during flood events, flood warning system for Chiang Mai city was set up in the form of flood hazard maps. Chiang Mai flood maps given by Civil Engineering Natural Disaster Research Unit (CENDRU) Chiang Mai University divides inundation areas into seven zones depending on upstream referenced water level at P1 (Chatchawan, 2005; CENDRU, 2013).

3.3 Parameter estimation for 1-D routing model

Figure 2 presents required hydraulic information at a cross section. Details of using these parameters for floodplain resistance model are presented in Appendix B: Flow resistance for one-dimensional over-bank flow in Jothityangkoon and Sivapalan (2003). Provided channel cross-section, measured rating curve at station P1 and channel bed slope, a Manning coefficient is estimated first by fitting the simulated with the observed rating curve, prior converting to the effective Chezy coefficient of the main channel (C_m). The Chezy coefficient in the flood plain is assumed to be the same as C_m.

3.4 Application of the model for flood extent estimation

Estimation procedures consist of four main steps (Figure 4).

(1) Formulate 1-D floodplain inundation model by fitting the simulated to observed flood extent maps based on assumed floodplain cross section (step 1-6 in Figure 4), upstream boundary condition and inputs are observed flood peaks at station P1.

(2) Convert input flood hydrograph to daily flood extent maps using 1-D flood routing model and flat water level assumption (step 7 in Figure 4).

(3) Simulate a time series of hourly flood extent maps by using 1D raster model (step 8-9 in Figure 4). After channel cross sections are converted to grid based-storage cells in series and given water surface elevation in main channel of the river, flow rates from Equation 1 and water surface elevations from Equation 2 are simultaneously calculated for each time step to generate water surface elevation on floodplain for each cross section. Upstream boundary condition and inputs are water surface elevations in the main channel at each cross section.

(4) Generate a pilot map of 3-D floodplain inundation extent 2-D raster model (step 10 in Figure 4). Similar to the
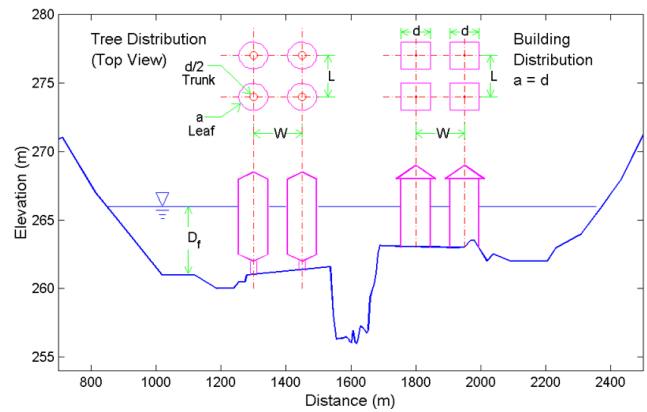
Figure 2. Required hydraulic information at a cross section, parameters for tree and building distribution on floodplain, L= W = 6-8 m (trees), = 10-15 m (building), a = 7-7.5 m (trees), = 9.5-12 m (building), d = 0.3-0.4 m (trees), = 9.5-12 m (building), and β = 0.2-0.5 (trees), = 0.4-0.8 (building).
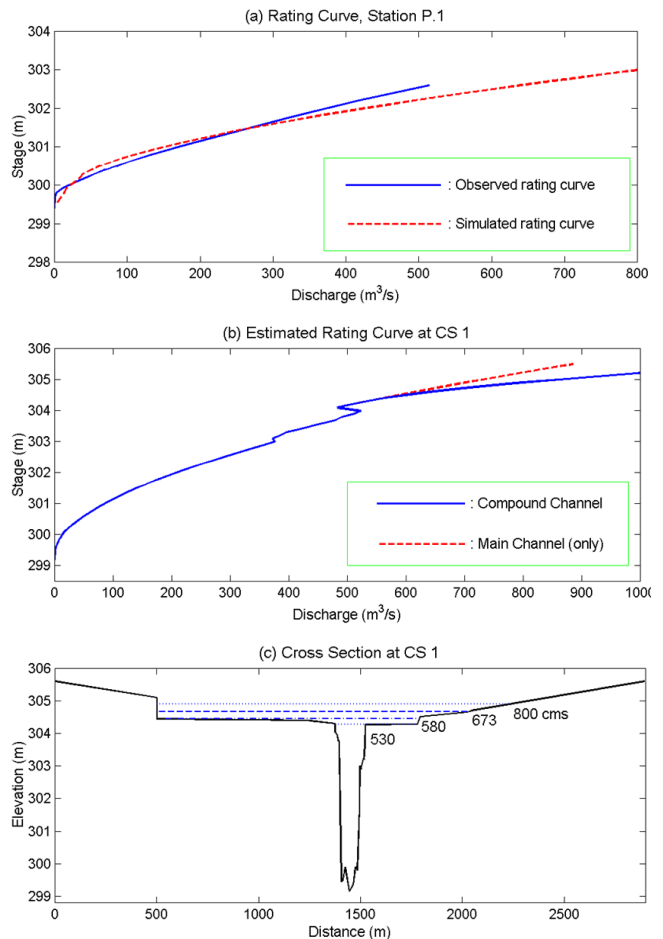
Figure 3. Steps to estimate flood extent at CS 1 (a) comparison of the measured and simulated rating curves for main channel at Station P1, (b) synthetic rating curve at CS 1, (c) estimated flood extents on both size of cross section at CS 1.

previous step, except the flow rates are determined on both directions (x: on floodplain, y: along main channel). Water surface elevation are generate for floodplain at each cross section and between cross sections.

3.5 Approach to estimate 3-D flood map

Hourly flood extent mapping from previous section is generated from the interpolation of water surface level from seven cross sections of floodplain. To test whether the raster models are able to simulate 2-D flood propagation over more realistic floodplain topography, grid-based storage cell from step 10 in Figure 4 is generated again from 1-D to 2-D in a short interval of a floodplain cross section.

4. Results and Discussion

4.1 Synthetic rating curves and flood extent for different water levels and flood peaks

Given surveyed cross section and channel slope of Ping River at stream gauge P1 (slope = 0.0087), simulated

Figure 4. Flowcharts for constructing a map of floodplain inundation extent.

rating curve fit to observed rating curve can be drawn with assumed Manning $n = 0.065$ for in-bank flow in main channel (Figure 3a). Figure 3b presents an example of estimated rating curves at cross section CS1 for two cases: (i) main channel only, (ii) compound channel including the effect of trees and/ or building distribution. The parameter m and k from calculated storage-discharge curve for seven cross sections are in the range of $m = 0.66$-0.72 (for main channel) 1.55-2.15 (for floodplain) and $k = 18417$-4536 (main channel) and 0.19-20.35 (floodplain).

The next cross section (CS1) is about 450 m downstream of P1 where there is no stream gauge; a synthetic rating curve is drawn by using n the same as P1 and surveyed cross sections from the profile and cross section surveying project along Ping River for Chiang Mai 's flood warning, completed in 2007 by the Royal Irrigation Department. The rating curve is extended to over-bank flows on floodplain based on trial and error processes until assumed shape of floodplain provides a good fit between estimated and observed flood extent and inundation depth in the form of flood inundation mapping (see Figure 4). Final shape of compound channel at CS1 is shown in Figure 3c. Over-bank flow occurs when Q>510 m^3/s. For Q = 530 m^3/s, water level, inundation extent from left and right river bank are 304.28, 1, and 255 m (line of sight toward downstream). The estimated distance of inundation extent for Q = 530 m^3/s can be plotted on the map in Figure 5b. Plan view of the flood map shows that there is no over-bank flow on the right bank of Ping River but over-bank is found on the left bank. Estimated and observed flood extents on the left bank are identical. Inundation extents for the other Qs are estimated and plotted in the flood map; see Figure 5c, d, e, and f. By using the method similar to CS1 step 1 to 6 in Figure 4, water level and inundation extent from the river bank are calculated for the other six cross sections (CS2-CS7) downstream of CS1. The estimated distant of inundation extent for all cross sections with the same Q is plotted in the same map to present the boundary and area of inundation cover. These maps present a good agreement between observed and simulated flood extent where the fit index is higher than 75%. Some discrepancies between estimated and observed inundation extent are found, for example, at CS2, Q = 580 m^3/s and at CS5, Q = 600 m^3/s, mostly are underestimations.

4.2 Daily flood extent mapping

Flood plain inundation modeling from a snap shot of inundation extent on floodplain can be used to simulate a time series of flood extent. Moderate daily flood events during 19-22 September 2005 with Q = 164, 543, 679 and 472 m^3/s are selected as an input to the proposed floodplain inundation model and used to generate daily floodplain inundation extents. Figure 6 presents a time series of daily flood map showing an expansion and contraction of flood extent along both sides of the Ping River. However, verification of these results with satellite images during this flood event is
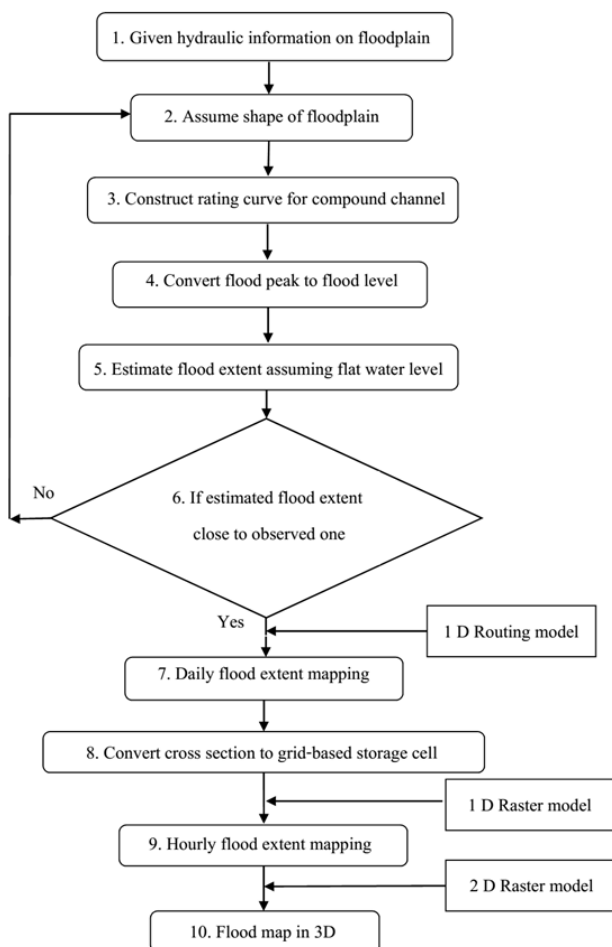
(a) 510 m³/s

(b) 530 m³/s

(c) 560 m³/s

(d) 580 m³/s
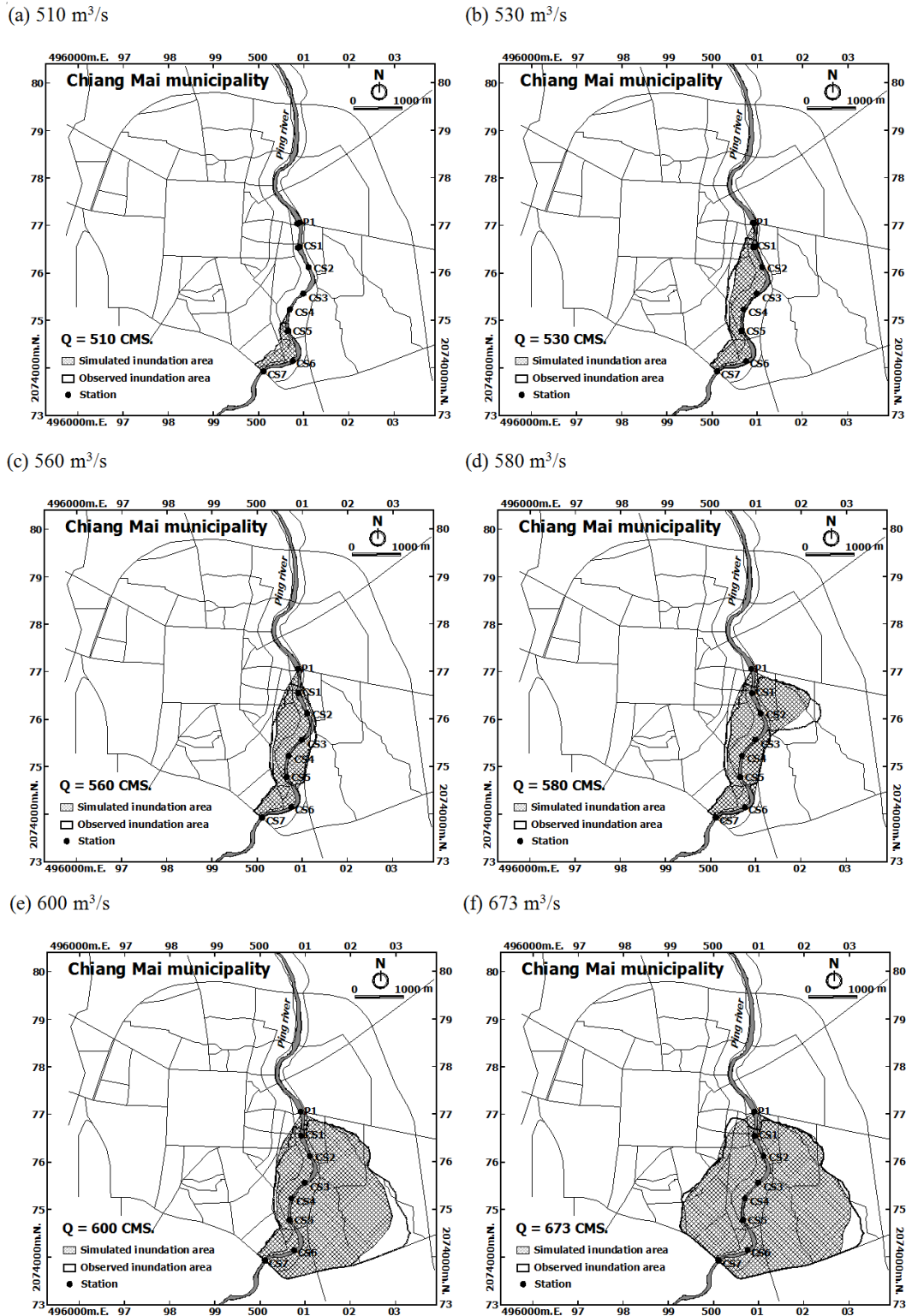
(e) 600 m³/s

(f) 673 m³/s

Figure 5. Comparison of observed and simulated flood inundation extent when flood peaks are (a) 510 m³/s, (b) 530 m³/s, (c) 560 m³/s, (d) 580 m³/s, (e) 600 m³/s, and (f) 673 m³/s

required. The results of flood routing model show that the simulated flood hydrograph from each river reaches are almost identical. This indicates that the attenuation of hydro-graph due to the effect of routing in short channel storages (3,850 m from P1 to CS7) with some lateral inflows is not significant.

(a) 20 September 2005 (543m³/s)

(b) 21 September 2005 (679m³/s)

(c)) 22 September 2005 (472m³/s)
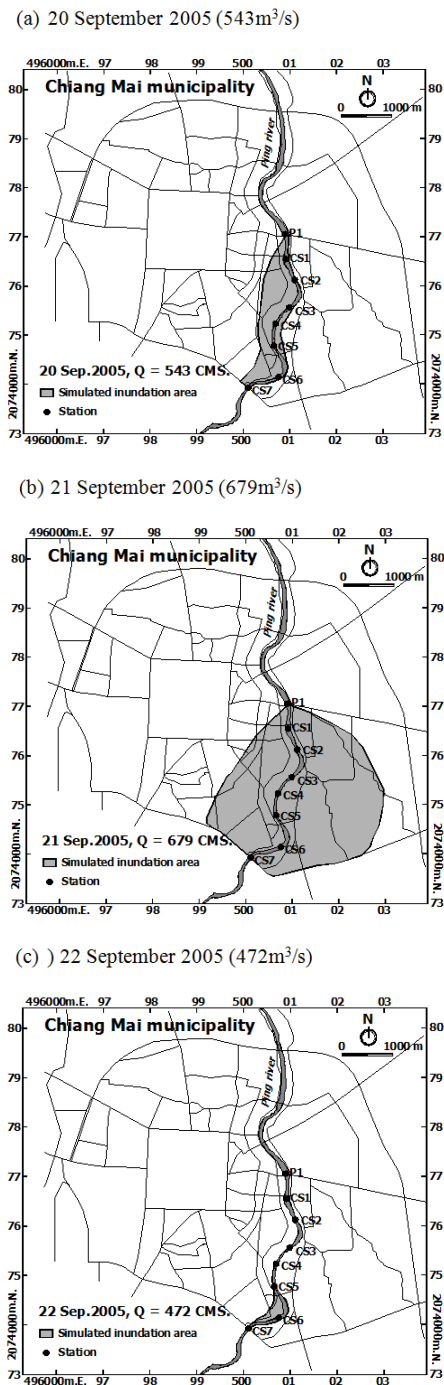
Figure 6. Simulation of daily flood inundation extent with (a) 20 September 2005 (543 m³/s), (b) 21 September 2005 (679 m³/s), (c) 22 September 2005 (472 m³/s).

4.3 Hourly flood extent mapping

4.3.1 Testing of raster model

Equations 1-6 were used to determine the water surface profile of encroached flood level by converting to MATLAB codes based on numerical approaches. The formu-

lation of 2 types of raster models was assessed through the tests of numerical exercises similar to Bates *et al.* (2010) as follow: Test 1: Flood wave propagation over a horizontal floodplain and comparison to an analytical solution; Test 2: Flood wave run-up on slope floodplain and comparison to a numerical solution; and Test 3: Tidal cycle of wetting and drying or rising and falling hydrograph on slope floodplain.

For the first test, using $u = 1$ ms^{-1}, $\Delta x = 50$ m, $\Delta t = 0.2$ s, $n = 0.01$ m$^{-1/3}$s to represent possible roughness on floodplain, total time = 3,600 s and maximum water level = 0.93 m, analytical solution from Equation 4 is presented in Figure 7a. Given initial condition, $h(t)$ at $x=0$ from Equation 4, the diffusive and inertial models can generate the water surface curve almost fit to the curve from analytical solution. The inertial model performs better than the diffusive model.

For the second test, there is no direct analytical solution. The solution of Equation 3 can be obtained by numerical method using 4th order Runge-Kutta method. The common parameter values for this test similar to Test 1, but including $S_0 = 10^{-3}$, $n = 0.09$ m$^{-1/3}$s, maximum water level = 8.5 m, $\Delta t = 0.05$ and 0.02 s for inertial and diffusive model, respectively. Maximum Δt is chosen to give no instability. Figure 7b shows estimated water surface elevation from the diffusive and inertial model compare to the numerical model.

For the third test, to investigate the simulation results from the whole cycle of flow reversals including rising front
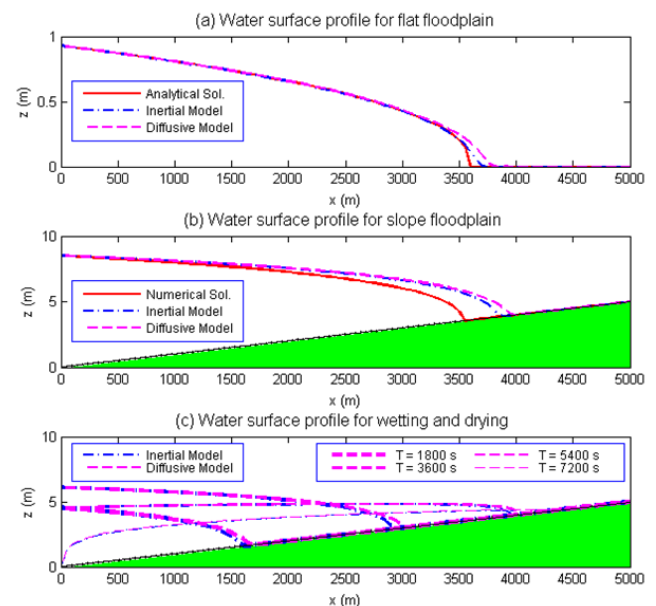
Figure 7. Testing results of raster model (a) simulated water surface elevation (z) at t = 3600 s and Δx = 50 m for wave propagation over a horizontal floodplain section using diffusive model, inertial model compare to analytical model, (b) z at t = 3,600 s and Δx = 50 m for wave propagation up an incline floodplain section using diffusive model, inertial model compare to numerical solution, (c) a time series of z at different time during wetting and drying for wave propagation up an incline floodplain section using diffusive model and inertial model.

of flood waves during floodplain wetting and recession front during floodplain drying, a sinusoidal wave boundary condition is used at $x = 0$, with wave amplitude 6.1 m period 4 hrs and $S_0 = 10^{-3}$ for simulation period 7,200 s. There is no analytical solution for this test. Only the difference between the inertial and diffusive model is investigated (Figure 7c).

4.3.2 Simulation of one dimensional hourly flood extent

Test 1 to 3 are series of idealized case with increasing complexity. To demonstrate the numerical performance of the raster model working over complex topography, surveyed data at each cross-section is interpolate to grid-based storage cell with fine spatial resolution $\Delta x = 50$ m. A time series of observed flood hydrograph (during 20-21 September 2005) is interpolated for selected time step with smooth shape transition from daily to hourly or smaller time step. Receiving these input hydrograph, the inertial and diffusive model can be used to simulate a time series of water surface profile (Figure 8). For a longer duration (48 hrs), the diffusive model generates distance of flood extent longer than the inertial model. At a corner of steep river banks, simulated water levels likely encroached into the river banks. This unrealistic water profile can be minimized if the resolution of Δx is decreased less than 50 m. The final step is the same as in Section 4.1, as the distance of inundation extent from all cross sections are combined to draw the map of time series of f loodplain inundation extents, as shown in Figure 9.

4.4 Flood extent in 3-D

A pilot test of 2-D grid-based storage cells are generated with a distance of 2,500 m along the Ping River downstream of CS6 and assuming an input flood level with constant depths of 0.95 m for the left bank and 1.20 m for the right bank, shown in Figure 10. This 3-D map shows a more realistic shape of flood wave propagation on the floodplain.
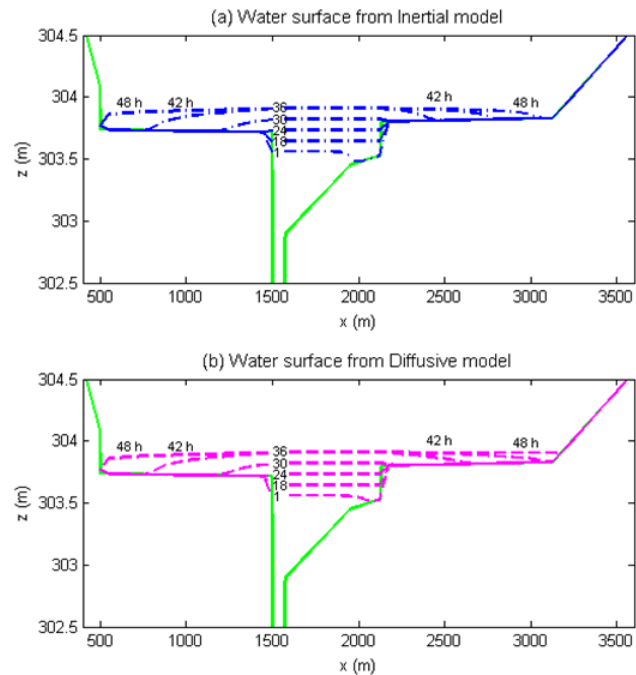
Figure 8. Simulated hourly flood levels at cross section No. 5 between 20 September 2005 to 21 September 2005.

The upper and lower surface represents propagated water surface and floodplain surface, respectively.

5. Conclusions

By using a synthetic rating curve for compound channel which includes the effect of trees and buildings distribution on floodplain, floodplain inundation model based on flat water surface assumption can be formulated with a number of selected channel cross sections. Although the vertical resolution of existing DEM (based on scale 1:50,000)
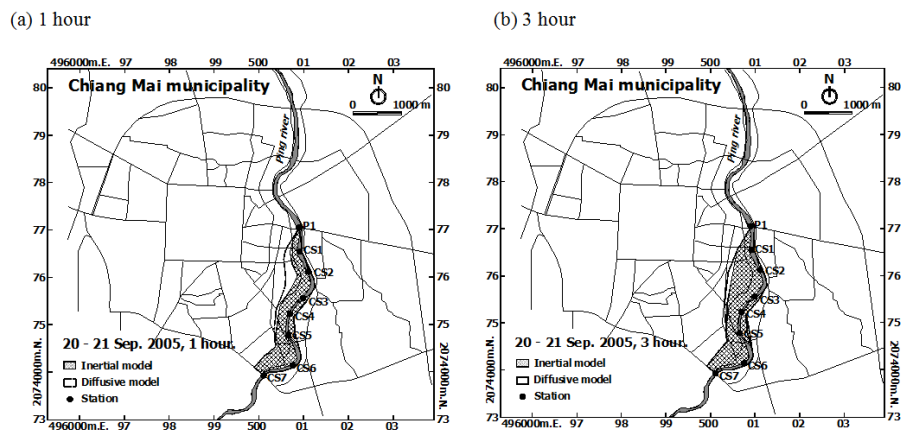
Figure 9. Comparison of simulated hourly flood map and inundation extent from inertial and diffusive model between 20-21 September 2005 with different simulation times (a) 1 hr, (b) 3 hrs, (c) 6 hrs, (d) 12 hrs, (e) 18 hrs, (f) 24 hrs, (g) 30 hrs, (h) 36 hrs, (i) 42 hrs, and (j) 48 hrs.

(c) 6 hour

(d) 12 hour

(e) 18 hour

(f) 24 hour

(g) 30 hour

(h) 36 hour

(i) 42 hours

(j) 48 hours
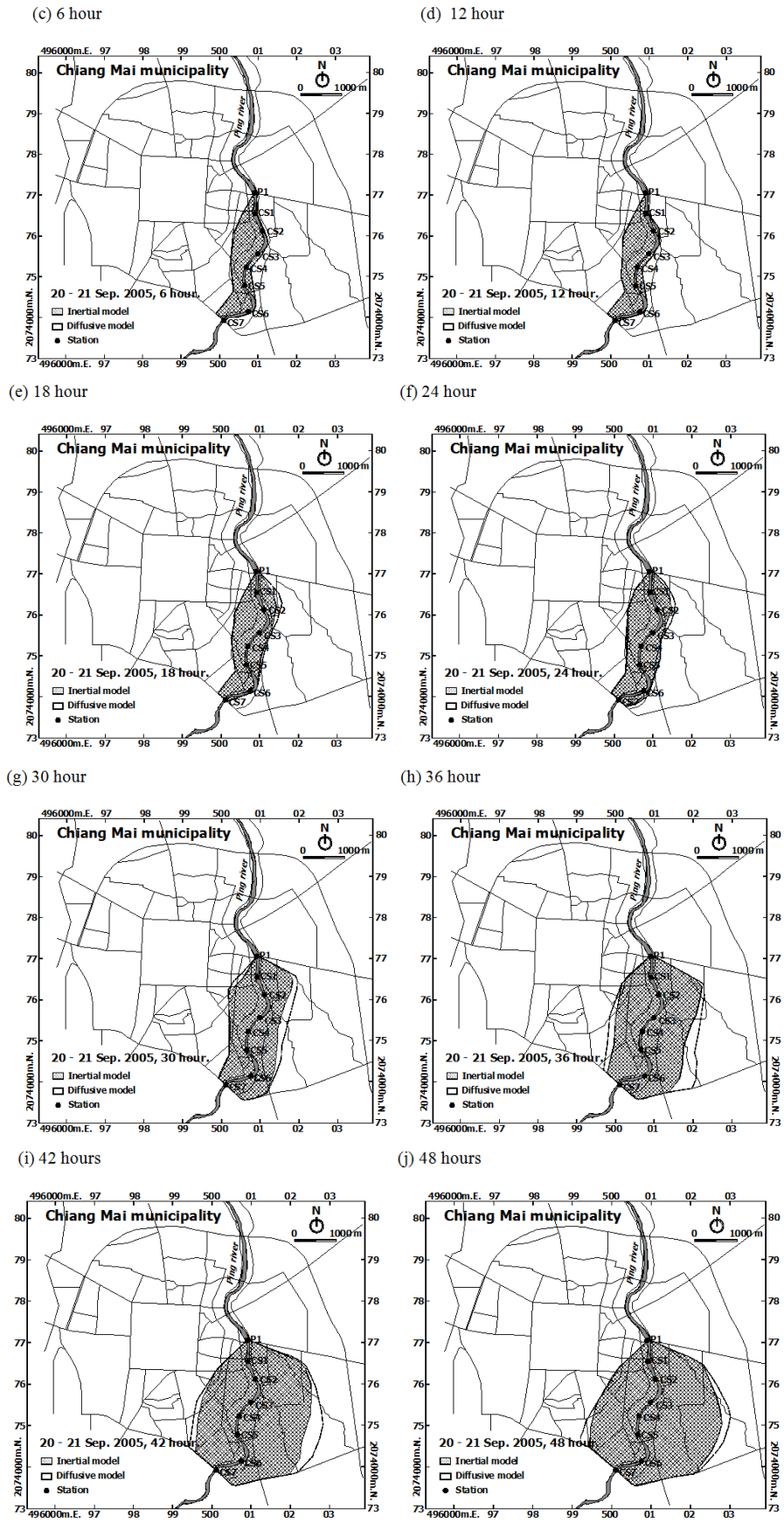
Figure 9.   Continued
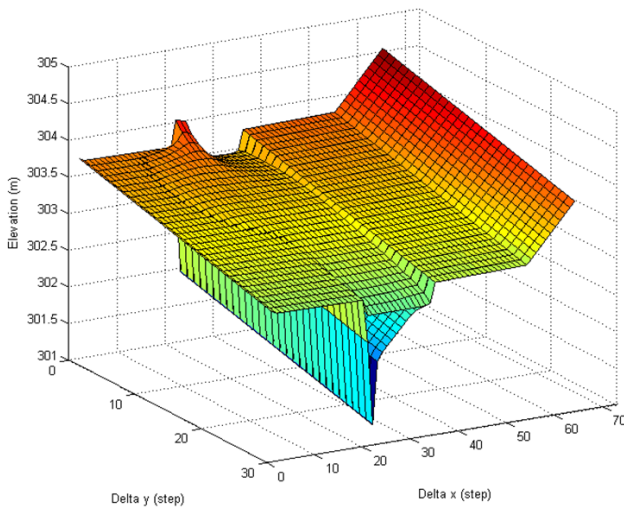
Figure 10. Simulated hourly flood inundation extent in 3-D map downstream of section CS6 generated from 2-D raster model (diffusion model) with 1,500 m length along the channel, slope = 0.0005, $n = 0.09$ m$^{-1/3}$s, $\Delta x = \Delta y = 50$ m, $\Delta t = 0.1$ s., Running time = 3 hrs.

for the floodplain of Chiang Mai Municipality is too low to represent any change of flood level, the assumed shape of floodplain can be defined and tested from a good fit between observed and simulated flood extent using the reverse engineering approach. This model can be used with confidence to construct a daily flood extent map.

To generate a time series of flood inundation maps from daily to hourly extents, a raster model consisting of diffusive and inertial formation are applied. The inertial model performs slightly better than the diffusive model for a horizontal floodplain and a slope floodplain, when compare to the analytical solution. The difference of simulated water level between the inertial and diffusive model become less pronounced for more complexity of floodplain topography and when receiving dynamic wetting and drying hydrograph. Inertial model can generate stable results with a time step larger than diffusive model due to increased stability with the addition of the inertial term. This study did not consider the computational performance and efficiency between different models.

If digital elevation data at a fine spatial resolution are available from an airborne laser altimetry survey or LiDAR data, then this data can be used to simulate more reliable inundation map and apply to the whole flooding area of Chiang Mai municipality, including the assessment of flood inundation extent from flood peaks with different exceedance probability or return period (Yin et al., 2013). The accuracy of flow patterns on floodplain depends on land surface characteristics and properties which can be interpreted from high resolution topographic information such as LiDAR data. This simplified floodplain inundation modeling are potential and alternative tools for developing countries where no spatial input data with high resolution are available.

References

Bates, P. D. and De Roo, A. P. J. 2000. A simple raster-based model for flood inundation simulation. Journal of Hydrology. 236, 54-77.

Bates, P. D., Horritt, M. S. and Fewtrell, T. J. 2010. A simple inertial formulation of the shallow water equations for efficient two-dimensional flood inundation modelling. Journal of Hydrology. 387, 33-45.

Bradbrook, K. F., Lane, S.N., Waller, S. G. and Bates, P.D. 2004. Two dimensional diffusion wave modelling of flood inundation using a simplified channel representation. International Journal River Basin Management. 2(3), 211–223.

CENDRU. 2013. General Information of the Upper Ping Basin (in Thai). Available from: http://cendru.eng.cmu.ac.th/flooding/?name=/chapter1/cp1_1/artical1 [April 5, 2013].

Chatchawan, S. 2005. Flood situation and flood protection report in Chiang Mai municipal area 2005 (in Thai). Proceedings of the Academic Conferences: Towards Society Harmony, Thai Development Research Institute Foundation, Chon Buri, Thailand, November 26-27, 2005.

Cook, A. and Merwade, V. 2009. Effect of topographic data, geometric configuration and modeling approach on flood inundation mapping. Journal of Hydrology. 377, 131-142.

De Kok, J. L. and Grossmann, M. 2010. Large-scale assessment of flood risk and the effects of mitigation measures along the Elbe River. Nature Hazards. 52, 143-166.

Ervine, D. A. and MacLeod, A. B. 1999. Modelling a river channel with distant floodbanks. Proceedings of the Institute of Civil Engineers, Water Maritime and Energy, 136(1), 21-33.

Fread, D. L. 1993. Flow routing (Chap. 10). In Handbook of Applied Hydrology, D.R. Maidment, editor. McGraw-Hill, New York, U.S.A.

Hagen, E., Shroder Jr., J. F., Lu, X. X. and Teufert, J. F. 2010. Reverse engineered flood hazard mapping in Afghanistan: A parsimonious flood map model for developing countries. Quaternary International. 226, 82-91.

Horritt, M. S. and Bates, P.D. 2002. Evaluation of 1D and 2D numerical models for predicting river flood inundation. Journal of Hydrology. 268(1), 87-99.

Hunter, N. H., Bates, P. D., Horritt, M. S. and Wilson, M. D. 2007. Simple spatially-distributed models for predicting flood inundation: a review. Geomorphology. 90, 208-225.

Hunter, N. H., Horritt, M. S., Bates, P. D., Wilson M. D. and Werner, M. G. F. 2005. An adaptive time step solution for raster-based storage cell modelling of floodplain inundation. Advances in Water Resources. 28, 975-991.

Jothityangkoon, C., Hirunteeyakul, C., Boonrawd, K. and Sivapalan, M. 2013. Assessing the impact of climate and land use changes on extreme floods in a large tropical catchment. Journal of Hydrology. 490, 88-105.

Jothityangkoon, C. and Sivapalan M. 2003. Towards estimation of extreme floods: examination of the roles of runoff process changes and floodplain flows. Journal of Hydrology. 281, 206-229.

IPCC, 2007. Climate Change 2007: The Scientific Basis, Cambridge University Press, Cambridge, U.K.

Merwade, V.M., Olivera, F., Arabi, M. and Edleman, S. 2008. Uncertainty in flood inundation mapping – current issues and future direction. ASCE Journal of Hydrologic Engineering. 13(7), 608-620.

Sarhadi, A., Soltani, S. and Modarres, R. 2012. Probabilistic flood inundation mapping of ungauged rivers: Linking GIS techniques and frequency analysis, Journal of Hydrology. 458-459, 68-86.

Tayefi, V., Lane, S. N., Hardy, R. J. and Yu, D. 2007. A comparison of one- and two-dimensional approaches to modelling flood inundation over complex upland floodplains. Hydrological Processes. 21(23), 3190-3202.

Yin, J., Yu, D., Yin, Z., Wang, J. and Xu, S. 2013. Multiple scenario analyses of Huangpu River flooding using a 1D/2D coupled flood inundation model. Natural Hazards. 66, 577-589.

Yu, D. and Lane S.N. 2006. Urban fluvial flood modelling using a two-dimensional diffusion wave treatment, part 1: Mesh resolution effects. Hydrological Processes. 20, 1541-1565.